International Tables for Crystallography (2006). Vol. B, Chapter 4.3, pp. 443–448.

4.3. Diffuse scattering in electron diffraction

BY J. M. COWLEY AND J. K. GJØNNES

4.3.1. Introduction

The origins of diffuse scattering in electron-diffraction patterns are the same as in the X-ray case: inelastic scattering due to electronic excitations, thermal diffuse scattering (TDS) from atomic motions, scattering from crystal defects or disorder. For diffraction by crystals, the diffuse scattering can formally be described in terms of a nonperiodic deviation $\Delta\varphi$ from the periodic, average crystal potential, $\bar{\varphi}$:

$$\varphi(\mathbf{r},t) = \bar{\varphi}(\mathbf{r}) + \Delta\varphi(\mathbf{r},t), \qquad (4.3.1.1)$$

where $\Delta\varphi$ may have a static component from disorder in addition to time-dependent fluctuations of the electron distribution or atomic positions.

In the kinematical case, the diffuse scattering can be treated separately. The intensity I_d as a function of the scattering variable $\mathbf{u}$ ($|\mathbf{u}| = 2\sin\theta/\lambda$) and energy transfer $h\nu$ is then given by the Fourier transform $\mathscr{F}$ of $\Delta\varphi$

$$I(\mathbf{u},\nu) = |\Delta\Phi(\mathbf{u}\nu)|^2 = |\mathscr{F}\{\Delta\varphi(\mathbf{r},t)\}|^2 = \mathscr{F}\{P_d(\mathbf{r},\nu)\} \quad (4.3.1.2)$$

and may also be written as the Fourier transform of a correlation function P_d representing fluctuations in space and time (see Cowley, 1981). When the energy transfers are small – as with TDS – and hence not measured, the observed intensity corresponds to an integral over ν:

$$I(\mathbf{u}) = I_d(\mathbf{u}) + I_{\rm av}(\mathbf{u})$$
$$I_d(\mathbf{u}) = \int I_d(\mathbf{u},\nu)\,\mathrm{d}\nu = \mathscr{F}\{P_d(\mathbf{r},\mathbf{0})\}$$

and also

$$I_d(\mathbf{u}) = \langle|\Phi(\mathbf{u})|^2\rangle - |\langle\Phi(\mathbf{u})\rangle|^2, \qquad (4.3.1.3)$$

where the brackets may indicate a time average, an expectation value, or a spatial average over the periodicity of the lattice in the case of static deviations from a periodic structure.

The considerations of TDS and static defects and disorder of Chapters 4.1 and 4.2 thus may be applied directly to electron diffraction in the kinematical approximation when the differences in experimental conditions and diffraction geometry are taken into account.

The most prominent contribution to the diffuse background in electron diffraction, however, is the inelastic scattering at low angles arising mainly from the excitation of outer electrons. This is quite different from the X-ray case where the inelastic ('incoherent') scattering, $S(\mathbf{u})$, goes to zero at small angles and increases to a value proportional to Z for high values of $|\mathbf{u}|$. The difference is due to the Coulomb nature of electron scattering, which leads to the kinematical intensity expression S/u^4, emphasizing the small-angle region. At high angles, the inelastic scattering from an atom is then proportional to Z/u^4, which is considerably less than the corresponding elastic scattering $(Z - f)^2/u^4$ which approaches Z^2/u^4 (Section 2.5.2) (see Fig. 4.3.1.1).

The kinematical description can be used for electron scattering only when the crystal is very thin (10 nm or less) and composed of light atoms. For heavy atoms such as Au or Pb, crystals of thickness 1 nm or more in principal orientations show strong deviations from kinematical behaviour. With increasing thickness, dynamical scattering effects first modify the sharp Bragg reflections and then have increasingly significant effects on the diffuse scattering. Bragg scattering of the diffuse scattering produces Kikuchi lines and other effects. Multiple diffuse scattering broadens the distribution and smears out detail. As the thickness increases further, the diffuse scattering increases and the Bragg beams are reduced in intensity until there is only a diffuse 'channelling pattern' where the features depend in only a very indirect way on the incident-beam direction or on the sources of the diffuse scattering (Uyeda & Nonoyama, 1968).

The multiple-scattering effects make the quantitative interpretation of diffuse scattering more difficult and complicate the extraction of particular components, *e.g.* disorder scattering. Much of the multiple scattering involves inelastic scattering processes. However, electrons that have lost energy of the order of 1 eV or more can be subtracted experimentally by use of electron energy filters (Krahl *et al.*, 1990; Krivanek *et al.*, 1992) which are commercially available. Measurement can be made also of the complete scattering function $I(\mathbf{u},\nu)$, but such studies have been rare. Another significant improvement to quantitative measurement of diffuse electron scattering is offered by new recording devices: slow-scan charge-couple-device cameras (Krivanek & Mooney, 1993) and imaging plates (Mori *et al.*, 1990).

There are some advantages in the use of electrons which make it uniquely valuable for particular applications.

(1) Diffuse-scattering distributions can be recorded from very small specimen regions, a few nm in diameter and a few nm thick. The diameter of the specimen area may be varied readily up to several μm.

(2) Diffraction information on defects or disorder may be correlated with high-resolution electron-microscope imaging of the same specimen area [see Section 4.3.8 in *IT* C (1999)].

(3) The electron-diffraction pattern approximates to a planar section of reciprocal space, so that complicated configurations of diffuse scattering may be readily visualized (see Fig. 4.3.1.2).

(4) Dynamical effects may be exploited to obtain information about localization of sources of the diffuse scattering within the unit cell.

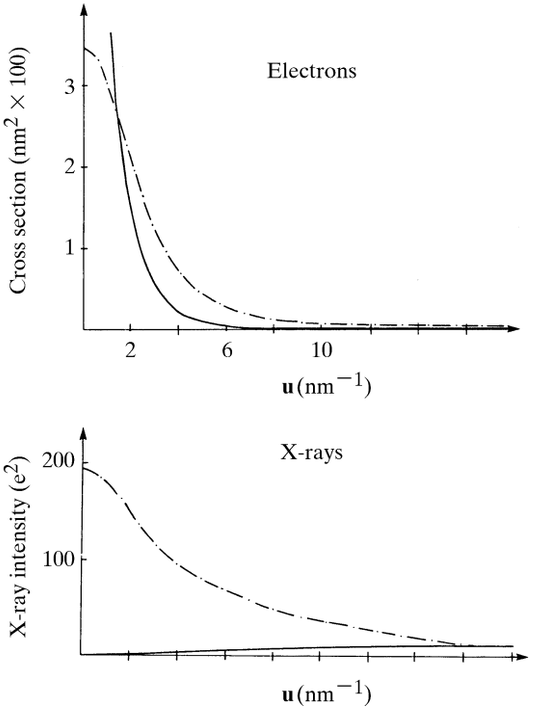

Fig. 4.3.1.1. Comparison between the kinematical inelastic scattering (full line) and elastic scattering (broken) for electrons and X-rays. Values for silicon [Freeman (1960) and *IT* C (1999)].

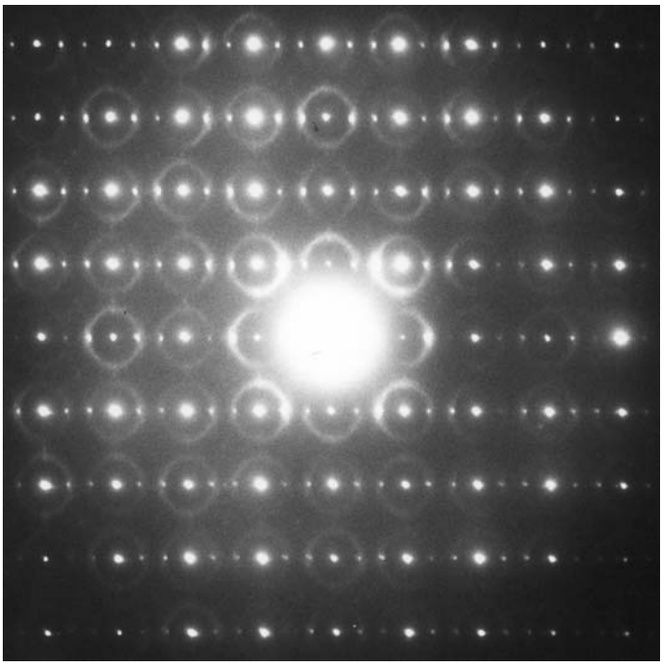

Fig. 4.3.1.2. Electron-diffraction pattern from a disordered crystal of $17Nb_2O_5.48WO_3$ close to the [001] orientation of the tetragonal tungsten-bronze-type structure (Iijima & Cowley, 1977).

These experimental and theoretical aspects of electron diffraction have influenced the ways in which it has been applied in studies of diffuse scattering.

In general, we may distinguish three different approaches to the interpretation of diffuse scattering:

(*a*) The crystallographic way, in which the Patterson- or correlation-function representation of the local order is emphasized, *e.g.* by use of short-range-order parameters.

(*b*) The physical model in terms of excitations. These are usually described in reciprocal (momentum) space: phonons, plasmons *etc.*

(*c*) Structure models in direct space. These must be derived by trial or by chemical considerations of bonds, coordinates *etc.*

Owing to the difficulties of separating the different components in the diffuse scattering, most work on diffuse scattering of electrons has followed one or both of the two last approaches, although Patterson-type interpretation, based upon kinematical scattering including some dynamical corrections, has also been tried.

4.3.2. Inelastic scattering

In the kinematical approximation, a general expression which includes inelastic scattering can be written in the form quoted by Van Hove (1954)

$$I(\mathbf{u},\nu) = \frac{m^3}{2^2h^6}\frac{k}{k_o} \times W(\mathbf{u}) \sum P_{n_o} \sum_{\eta} \sum_{j=1}^{Z} |\langle n_o| \exp\{2\pi i \mathbf{u}\cdot\mathbf{R}_j\}|n\rangle|^2 \times \delta\left(\nu + \frac{E_n - E_{n_o}}{h}\right) \quad (4.3.2.1)$$

for the intensity of scattering as function of energy transfer and momentum transfer from a system of Z identical particles, $\mathbf{R}_j$. Here m and h have their usual meanings; k_o and k, E_{n_o} and E_n are wavevectors and energies before and after the scattering between object states n_o and n; P_{n_o} are weights of the initial states; $W(\mathbf{u})$ is a form factor (squared) for the individual particle.

In equation (4.3.2.1), $\mathbf{u}$ is essentially momentum transfer. When the energy transfer is small ($\Delta E/E \ll \theta$), we can still write $|\mathbf{u}| = 2\sin\theta/\lambda$, then the sum over final states n is readily performed and an expression of the Waller–Hartree type is obtained for the total inelastic scattering as a function of angle:

$$I_{\text{inel}}(\mathbf{u}) \propto \frac{S}{u^4},$$

where

$$S(u) = Z - \sum_{j=1}^{Z} |f_{jj}(u)|^2 - \sum_{j}^{Z}\sum_{\neq k}^{Z} |f_{jk}(u)|^2, \quad (4.3.2.2)$$

and where the one-electron f's for Hartree–Fock orbitals, $f_{jk}(\mathbf{u}) = \langle j|\exp(2\pi i\mathbf{u}\cdot\mathbf{r})|k\rangle$, have been calculated by Freeman (1959, 1960) for atoms up to $Z = 30$. The last sum is over electrons with the same spin only.

The Waller–Hartree formula may be a very good approximation for Compton scattering of X-rays, where most of the scattering occurs at high angles and multiple scattering is no problem. With electrons, it has several deficiencies. It does not take into account the electronic structure of the solid, which is most important at low values of u. It does not include the energy distribution of the scattering. It does not give a finite cross section at zero angle, if u is interpreted as an angle. In order to remedy this, we should go back to equation (4.3.1.2) and decompose $\mathbf{u}$ into two components, one tangential part which is associated with angle in the usual way and one normal component along the beam direction, u_n, which may be related to the excitation energy $\Delta E = E_n - E_{n_o}$ by the expression $u_n = \Delta E_k/2E$. This will introduce a factor $1/(u^2 + u_n^2)$ in the intensity at small angles, often written as $1/(\theta^2 + \theta_E^2)$, with ΔE estimated from ionization energies *etc.* (Strictly speaking, ΔE is not a constant, not even for scattering from one shell. It is a weighted average which will vary with u.)

Calculations beyond this simple adjustment of the Waller–Hartree-type expression are few. Plasmon scattering has been treated on the basis of a nearly free electron model by Ferrel (1957):

$$\frac{\mathrm{d}^2\sigma}{\mathrm{d}(\Delta E)\,\mathrm{d}\Omega} = (1/\pi^2 a_H m v^2 N)(-\mathrm{Im}\{1/\varepsilon\})/(\theta^2 + \theta_E^2), \quad (4.3.2.3)$$

where m, v are relativistic mass and velocity of the incident electron, N is the density of the valence electrons and $\varepsilon(\Delta E, \theta)$ their dielectric constant. Upon integration over ΔE:

$$\frac{\mathrm{d}\sigma}{\mathrm{d}\Omega} = \frac{E_p}{2\pi a_H m v N}[1/(\theta^2 + \theta_E^2)G(\theta,\theta_c)], \quad (4.3.2.4)$$

where $G(\theta,\theta_c)$ takes account of the cut-off angle Θ_c. Inner-shell excitations have been studied because of their importance to spectroscopy. The most realistic calculations may be those of Leapman *et al.* (1980) where one-electron wavefunctions are determined for the excited states in order to obtain 'generalized oscillator strengths' which may then be used to modify equation (4.3.1.2).

At high energies and high momentum transfer, the scattering will approach that of free electrons, *i.e.* a maximum at the so-called Bethe ridge, $E = h^2u^2/2m$.

A complete and detailed picture of inelastic scattering of electrons as a function of energy and angle (or scattering variable) is lacking, and may possibly be the least known area of diffraction by solids. It is further complicated by the dynamical scattering, which involves the incident and diffracted electrons and also the ejected atomic electron (see *e.g.* Maslen & Rossouw, 1984).

4.3.3. Kinematical and pseudo-kinematical scattering

Kinematical expressions for TDS or defect and disorder scattering according to equation (4.3.1.3) can be obtained by inserting the appropriate atomic scattering factors in place of the X-ray scattering factors in Chapter 4.1. The complications introduced by dynamical diffraction are considerable (see Section 4.3.4). In the most general case, a complete specification of the disordered structure may be needed. However, for thin specimens, approximate treatments of the deviations from kinematical scattering may lead to relatively simple forms. Two such cases are treated in this section, both relying on the small-angle nature of electron scattering. The first is based upon the phase-object approximation, which applies to small angles and thin specimens.

The amplitude at the exit surface of a specimen can always be written as a sum of a periodic and a nonperiodic part, and may in analogy with the kinematical case [equation (4.3.1.1)] be written

$$\psi(\mathbf{r}) = \bar{\psi}(\mathbf{r}) + \Delta\psi(\mathbf{r}), \tag{4.3.3.1}$$

where $\mathbf{r}$ is a vector in two dimensions. The intensities can be separated in the same way [*cf.* equation (4.3.1.3)].

When the phase-object approximation applies (Chapter 2.1)

$$\begin{aligned}\psi(\mathbf{r}) &= \exp\{-i\sigma\varphi(\mathbf{r})\} \\ &= \exp\{-i\sigma\bar{\varphi}(\mathbf{r})\}[1 - i\sigma\Delta\varphi(\mathbf{r}) - \ldots].\end{aligned} \tag{4.3.3.2}$$

Then the Bragg reflections are given by Fourier transform of the periodic part, *viz*:

$$\langle\exp\{-i\sigma\varphi(\mathbf{r})\}\rangle = \exp\{-i\sigma\bar{\varphi}(\mathbf{r})\}\exp\{-\tfrac{1}{2}\sigma^2\langle\Delta\varphi^2(\mathbf{r})\rangle\}; \tag{4.3.3.3}$$

note that an absorption function is introduced.

The diffuse scattering derives from

$$-i\sigma\Delta\varphi(\mathbf{r})\exp\{-i\sigma\bar{\varphi}(\mathbf{r})\}, \tag{4.3.3.4}$$

so that

$$I_d(\mathbf{u}) = \sigma^2|\Delta\Phi(\mathbf{u}) * \Phi_{\rm av}(\mathbf{u})|^2. \tag{4.3.3.5}$$

Thus, the kinematical diffuse-scattering amplitude is convoluted with the amplitude function for the average structure, *i.e.* the set of sharp Bragg beams. When the direct beam, $\Phi_{\rm av}(0)$, is relatively strong, the kinematical diffuse scattering will be modified to only a limited extent by convolution with the Bragg reflections. To the extent that the diffuse scattering is periodic in reciprocal space, the effect will be to modify the intensity by a slowly varying function. Thus the shapes of local diffuse maxima will not be greatly affected.

The electron-microscope image contrast derived from the diffuse scattering will be obtained by inserting equation (4.3.3.4) in the appropriate intensity expressions of Section 4.3.8 of *IT* C (1999).

Another approach may be used for extended crystal defects in thin films, *e.g.* faults normal or near-normal to the film surface. Often, an average periodic structure may not readily be defined, as in the case of a set of incommensurate stacking faults. Kinematically, the projection of the structure in the simplest case may be described by convoluting the projection of a unit-cell structure with a nonperiodic set of delta functions which constitute a distribution function:

$$\varphi(\mathbf{r}) = \varphi_0(\mathbf{r}) * \sum_n \delta(\mathbf{r} - \mathbf{r}_n) = \varphi_0(\mathbf{r}) * \mathrm{d}(\mathbf{r}). \tag{4.3.3.6}$$

Then the diffraction-pattern intensity is

$$I(\mathbf{u}) = |\Phi_0(\mathbf{u})|^2|D(\mathbf{u})|^2. \tag{4.3.3.7}$$

Here, $\Phi_0(\mathbf{u})$ is the scattering amplitude of the unit whereas the function $|D(\mathbf{u})|^2$, where $D(\mathbf{u}) = \mathscr{F}\{d(\mathbf{r})\}$, gives the configuration of spots, streaks or other diffraction maxima corresponding to the faulted structure (see *e.g.* Marks, 1985).

In the projection (column) approximation to dynamical scattering, the wavefunction at the exit surface may be given by an expression identical to (4.3.3.6), but with a wavefunction, $\psi_0(\mathbf{r})$, for the unit in place of the projected potential, $\varphi_0(\mathbf{r})$.

An intensity expression of the same form as (4.3.3.7) then applies, with a dynamical scattering amplitude Ψ_0 for the scattering unit substituted for the kinematical amplitude Φ_0.

$$I(\mathbf{u}) = |\Psi_0(\mathbf{u})|^2|D(\mathbf{u})|^2, \tag{4.3.3.8}$$

which in the simplest case describes a diffraction pattern with the same features as in the kinematical case. Note that $\Psi_0(\mathbf{u})$ may have different symmetries when the incident beam is tilted away from a zone axis, leading to diffuse streaks *etc.* appearing also in positions where the kinematical diffuse scattering is zero. More complicated cases have been considered by Cowley (1976*a*) who applied this type of analysis to the case of nonperiodic faulting in magnesium fluorogermanate (Cowley, 1976*b*).

4.3.4. Dynamical scattering: Bragg scattering effects

The distribution of diffuse scattering is modified by higher-order terms in essentially two ways: Bragg scattering of the incident and diffuse beams or multiple diffuse scattering, or by a combination.

Theoretical treatment of the Bragg scattering effects in diffuse scattering has been given by many authors, starting with Kainuma's (1955) work on Kikuchi-line contrast (Howie, 1963; Fujimoto & Kainuma, 1963; Gjønnes, 1966; Rez *et al.*, 1977; Maslen & Rossouw, 1984; Wang, 1995; Allen *et al.*, 1997). Mathematical formalism may vary but the physical pictures and results are essentially the same. They may be discussed with reference to a Born-series expansion, *i.e.* by introducing the potential φ in the integral equation, as a sum of a periodic and a nonperiodic part [*cf.* equation (4.3.1.1)] and arranging the terms by orders of $\Delta\varphi$.

$$\begin{aligned}\psi &= \psi_0 + G\varphi\psi \\ &= [1 + G\varphi + (G\varphi)^2 + \ldots]\psi_0 \\ &= [1 + G\bar{\varphi} + (G\bar{\varphi})^2 + \ldots]\psi_0 \\ &\quad + [1 + G\bar{\varphi} + (G\bar{\varphi})^2 + \ldots] \\ &\quad \times G(\Delta\varphi)[1 + G\bar{\varphi} + (G\bar{\varphi})^2 + \ldots]\psi_0 \\ &\quad + \text{higher-order terms.}\end{aligned} \tag{4.3.4.1}$$

Some of the higher-order terms contributing to the Bragg scattering can be included by adding the essentially imaginary term $\langle\Delta\varphi G(\Delta\varphi)\rangle$ to the static potential $\bar{\varphi}$.

Theoretical treatments have mostly been limited to the first-order diffuse scattering. With the usual approximation to forward scattering, the expression for the amplitude of diffuse scattering in a direction $\mathbf{k}_0 + \mathbf{u} + \mathbf{g}$ can be written as

$$\begin{aligned}\psi(\mathbf{u} + \mathbf{g}) = \sum_g\sum_f \int_0^z & S_{hg}(\mathbf{k}_0 + \mathbf{u}, z - z_1) \\ & \times \Delta\Phi(\mathbf{u} + \mathbf{g} - \mathbf{f})S_{f0}(\mathbf{k}_0, z_1)\,\mathrm{d}z_1\end{aligned} \tag{4.3.4.2}$$

and read (from right to left): S_{f0}, Bragg scattering of the incident beam above the level z_1; $\Delta\Phi$, diffuse scattering within a thin layer $\mathrm{d}z_1$ through the Fourier components $\Delta\Phi$ of the nonperiodic potential $\Delta\Phi$; S_{hg}, Bragg scattering between diffuse beams in the lower part of the crystal. It is commonly assumed that diffuse scattering at different levels can be treated as independent (Gjønnes, 1966), then the intensity expression becomes

$$I(\mathbf{u}+\mathbf{g}) = \sum_h \sum_{h'} \sum_f \sum_{f'} \int_0^z S_{gh}(2) S^*_{gh'}(2) \times \langle \Delta\Phi(\mathbf{u}+\mathbf{h}-\mathbf{f}) \Delta\Phi^*(\mathbf{u}+\mathbf{h}'-\mathbf{f}') \rangle \times S_{f0}(1) S^*_{f'0}(1)\, \mathrm{d}z_1, \quad (4.3.4.3)$$

where (1) and (2) refer to the regions above and below the diffuse-scattering layer. This expression can be manipulated further, *e.g.* by introducing Bloch-wave expansion of the scattering matrices, *viz*

$$I(\mathbf{u}+\mathbf{g}) = \sum_{hh'} \sum_{ff'} \sum_{jj'} \sum_{ii'} C^j_g(2) C^{j'*}_g(2) C^{j*}_h(2) C^{j'}_{h'}(2) \times \frac{\exp[i(\gamma^i - \gamma^{i'})z] - \exp[i(\gamma^j - \gamma^{j'})z]}{\gamma^i - \gamma^{i'} - \gamma^j + \gamma^{j'}} \times \langle f(\mathbf{u}+\mathbf{h}-\mathbf{f}) f^*(\mathbf{u}+\mathbf{h}'-\mathbf{f}') \rangle \times C^{i*}_f(1) C^{i'}_{f'}(1) C^i_0(1) C^{i*}_0(1), \quad (4.3.4.4)$$

which may be interpreted as scattering by $\Delta\varphi$ between Bloch waves belonging to the same branch (intraband scattering) or different branches (interband scattering). Another alternative is to evaluate the scattering matrices by multislice calculations (Section 4.3.5).

Expressions such as (4.3.4.2) contain a large number of terms. Unless very detailed calculations relating to a precisely defined model are to be carried out, attention should be focused on the most important terms.

In Kikuchi-line contrast, the scattering in the upper part of the crystal is usually not considered and frequently the angular variation of the $\Phi(\mathbf{u})$ is also neglected. In diffraction contrast from small-angle inelastic scattering, it may be sufficient to consider the intraband terms [$i = i'$, $j = j'$ in (4.3.4.3)].

In studies of diffuse-scattering distribution, the factor $\langle \Phi(\mathbf{u}+\mathbf{h}) \Phi(\mathbf{u}+\mathbf{h}') \rangle$ will produce two types of terms: Those with $\mathbf{h} = \mathbf{h}'$ result only in a redistribution of intensity between corresponding points in the Brillouin zones, with the same total intensity. Those with $\mathbf{h} \neq \mathbf{h}'$ lead to enhancement or reduction of the total diffuse intensity and hence absorption from the Bragg beam and enhanced/reduced intensity of secondary radiation, *i.e.* anomalous absorption and channelling effects. They arise through interference between different Fourier components of the diffuse scattering and carry information about position of the sources of diffuse scattering, referred to the projected unit cell. This is exploited in channelling experiments, where beam direction is used to determine atom reaction (Taftø & Spence, 1982; Taftø & Lehmpfuhl, 1982).

Gjønnes & Høier (1971) expressed this information in terms of the Fourier transform R of the generalized or Kikuchi-line form factor;

$$\langle \Delta\Phi(\mathbf{u}) \Delta\Phi^*(\mathbf{u}+\mathbf{h}) \rangle \mathbf{u}^2(\mathbf{u}+\mathbf{h})^2 = Q(\mathbf{u}+\mathbf{h}) = \mathscr{F}\{R(\mathbf{r},\mathbf{g})\} \quad (4.3.4.5)$$

includes information both about correlations between sources of diffuse scattering and about their position in the projected unit cell. It is seen that $Q(\mathbf{u},0)$ represents the kinematical intensity, hence $\int R(\mathbf{r},\mathbf{g})\, \mathrm{d}\mathbf{g}$ is the Patterson function. The integral of $Q(\mathbf{u},\mathbf{h})$ in the plane gives the anomalous absorption (Yoshioka, 1957) which is related to the distribution $R(\mathbf{r},0)$ of scattering centres across the unit cell.

The scattering factor $\langle \Delta\Phi(\mathbf{u}) \Delta\Phi^*(\mathbf{u}-\mathbf{h}) \rangle$ can be calculated for different modes. For one-electron excitations as an extension of the Waller–Hartree expression (Gjønnes, 1962; Whelan, 1965):

$$\langle \Delta\Phi(\mathbf{u}) \Delta\Phi^*(\mathbf{u}-\mathbf{h}) \rangle = \sum_i \frac{f_{ii}(\mathbf{h}) - f_{ii}(\mathbf{u}) f_{ii}(|\mathbf{h}-\mathbf{u}|)}{u^2(\mathbf{h}-\mathbf{u})^2} - \sum_i \sum_{i \neq j} \frac{f_{ij}(\mathbf{u}) f_{ij}(|\mathbf{h}-\mathbf{u}|)}{u^2(\mathbf{h}-\mathbf{u})^2}, \quad (4.3.4.6)$$

where f_{ij} are the one-electron amplitudes (Freeman, 1959).

A similar expression for scattering by phonons is obtained in terms of the scattering factors $G_j(\mathbf{u},\mathbf{g})$ for the branch j, wavevector $\mathbf{g}$ and a polarization vector $\mathbf{l}_{j,q}$ (see Chapter 4.1):

$$\langle \Delta\Phi(\mathbf{u}) \Delta\Phi^*(\mathbf{u}-\mathbf{h}) \rangle = G_j(\mathbf{u},\mathbf{q}) G^*_j(\mathbf{u}-\mathbf{h},\mathbf{q}), \quad (4.3.4.7)$$

independent phonons being assumed.

For scattering from substitutional order in a binary alloy with ordering on one site only, we obtain simply

$$\Delta\Phi(\mathbf{u}) \Delta\Phi^*(\mathbf{u}-\mathbf{h}) = |\Delta\varphi(\mathbf{u})|^2 \frac{f_A(|\mathbf{u}-\mathbf{h}|) - f_B(|\mathbf{u}-\mathbf{h}|)}{f_A(\mathbf{u}) - f_B(\mathbf{u})}, \quad (4.3.4.8)$$

where $f_{A,B}$ are atomic scattering factors. It is seen that $Q(\mathbf{u})$ then does not contain any new information; the location of the site involved in the ordering is known.

When several sites are involved in the ordering, the dynamical scattering factor becomes less trivial, since scattering factors for the different ordering parameters (for different sites) will include a factor $\exp(2\pi i \mathbf{r}_m \cdot \mathbf{h})$ (see Andersson *et al.*, 1974).

From the above expressions, it is found that the Bragg scattering will affect diffuse scattering from different sources differently: Diffuse scattering from substitutional order will usually be enhanced at low and intermediate angles, whereas scattering from thermal and electronic fluctuations will be reduced at low angles and enhanced at higher angles. This may be used to study substitutional order and displacement order (size effect) separately (Andersson, 1979).

The use of such expressions for quantitative or semiquantitative interpretation raises several problems. The Bragg scattering effects occur in all diffuse components, in particular the inelastic scattering, which thus may no longer be represented by a smooth, monotonic background. It is best to eliminate this experimentally. When this cannot be done, the experiment should be arranged so as to minimize Kikuchi-line excess/deficient terms, by aligning the incident beam along a not too dense zone. In this way, one may optimize the diffuse-scattering information and minimize the dynamical corrections, which then are used partly as guides to conditions, partly as refinement in calculations.

The multiple scattering of the background remains as the most serious problem. Theoretical expressions for multiple scattering in the absence of Bragg scattering have been available for some time (Moliere, 1948), as a sum of convolution integrals

$$I(\mathbf{u}) = [(\mu t) I_1(\mathbf{u}) + (1/2)(\mu t)^2 I_2(\mathbf{u}) + \ldots] \exp(-\mu t), \quad (4.3.4.9)$$

where $I_2(\mathbf{u}) = I_1(\mathbf{u}) * I_1(\mathbf{u}) \ldots$ *etc.*, and $I_1(\mathbf{u})$ is normalized.

A complete description of multiple scattering in the presence of Bragg scattering should include Bragg scattering between diffuse scattering at all levels z_1, z_2, *etc.* This quickly becomes unwieldy. Fortunately, the experimental patterns seem to indicate that this is not necessary: The Kikuchi-line contrast does not appear to be very sensitive to the exact Bragg condition of the incident beam. Høier (1973) therefore introduced Bragg scattering only in the last part of the crystal, *i.e.* between the level z_n and the final thickness z for n-times scattering. He thus obtained the formula:

$$I(\mathbf{u}+\mathbf{h}) = \sum_j |C_h^j|^2 \left\{ A_1^j \sum_g \sum_{\neq g'} F_1(\mathbf{u},\mathbf{g},\mathbf{g}') C_g^j C_{g'}^{j*} + \sum_n \sum_g A_{ng}^j F_n(\mathbf{u},\mathbf{g}) |C_g^j|^2 \right\}, \quad (4.3.4.10)$$

where F_n are normalized scattering factors for nth-order multiple diffuse scattering and A_n^j are multiple-scattering coefficients which include absorption.

When the thickness is increased, the variation of $F_n(\mathbf{u},\mathbf{g})$ with angle becomes slower, and an expression for intensity of the channelling pattern is obtained (Gjønnes & Taftø, 1976):

$$I(\mathbf{u}+\mathbf{h}) = \sum_j \sum_g \sum_n |C_h^j|^2 |C_g^j|^2 A_n^j = \sum_j |C_h^j|^2 \sum_n A_n^j \rightarrow |C_h^j|^2/\mu^j(\mathbf{u}). \quad (4.3.4.11)$$

Another approach is the use of a modified diffusion equation (Ohtsuki *et al.*, 1976).

These expressions seem to reproduce the development of the general background with thickness over a wide range of thicknesses. It may thus appear that the contribution to the diffuse background from known sources can be treated adequately – and that such a procedure must be included together with adequate filtering of the inelastic component in order to improve the quantitative interpretation of diffuse scattering.

4.3.5. Multislice calculations for diffraction and imaging

The description of dynamical diffraction in terms of the progression of a wave through successive thin slices of a crystal (Chapter 5.2) forms the basis for the multislice method for the calculation of electron-diffraction patterns and electron-microscope images [see Section 4.3.6.1 in *IT* C (1999)]. This method can be applied directly to the calculations of diffuse scattering in electron diffraction due to thermal motion and positional disorder and for calculating the images of defects in crystals.

It is essentially an amplitude calculation based on the formulation of equation (4.3.4.1) [or (4.3.4.2)] for first-order diffuse scattering. The Bragg scattering in the first part of the crystal is calculated using a standard multislice method for the set of beams **h**. In the nth slice of the crystal, a diffuse-scattering amplitude $\Psi_d(\mathbf{u})$ is convoluted with the incident set of Bragg beams. For each **u**, propagation of the set of beams $\mathbf{u}+\mathbf{h}$ is then calculated through the remaining slices of the crystal. The intensities for the exit wave at the set of points $\mathbf{u}+\mathbf{h}$ are then calculated by adding either amplitudes or intensities. Amplitudes are added if there is correlation between the defects in successive slices. Intensities are added if there are no such correlations. The process is repeated for all **u** values to obtain a complete mapping of the diffuse scattering.

Calculations have been made in this way, for example, for short-range order in alloys (Fisher, 1969) and also for TDS on the assumption of both correlated and uncorrelated atomic motions (Doyle, 1969). The effects of the correlations were shown to be small.

This computing method is not practical for electron-microscope images in which individual defects are to be imaged. The perturbations of the exit wavefunction due to individual defects (vacancies, replaced atoms, displaced atoms) or small groups of defects may then be calculated with arbitrary accuracy by use of the 'periodic continuation' form of the multislice computer programs in which an artificial, large, superlattice unit cell is assumed [Section 4.3.6.1 in *IT* C (1999)]. The corresponding images and micro-diffraction patterns from the individual defects or clusters may then be calculated (Fields & Cowley, 1978). A more recent discussion of the image calculations, particularly in relation to thermal diffuse scattering, is given by Cowley (1988).

In order to calculate the diffuse-scattering distributions from disordered systems or from a crystal with atoms in thermal motion by the multislice method with periodic continuation, it would be necessary to calculate for a number of different defect configurations sufficiently large to provide an adequate representation of the statistics of the disordered system. However, it has been shown by Cowley & Fields (1979) that, if the single-diffuse-scattering approximation is made, the perturbations of the exit wave due to individual defects are characteristic of the defect type and of the slice number and may be added, so that a considerable simplification of the computing process is possible. Methods for calculating diffuse scattering in electron-diffraction patterns using the multislice approach are described by Tanaka & Cowley (1987) and Cowley (1989). Loane *et al.* (1991) introduced the concept of 'frozen phonons' for multislice calculations of thermal scattering.

4.3.6. Qualitative interpretation of diffuse scattering of electrons

Quantitative interpretation of the intensity of diffuse scattering by calculation of *e.g.* short-range-order parameters has been the exception. Most studies have been directed to qualitative features and their variation with composition, treatment *etc.* Many features in the scattering which pass unrecognized in extensive X-ray or neutron investigations will be observed readily with electrons, frequently inviting other ways of interpretation.

Most such studies have been concerned with substitutional disorder, but the extensive investigations of thermal streaks by Honjo and co-workers should be mentioned (Honjo *et al.*, 1964). Diffuse spots and streaks from disorder have been observed from a wide range of substances. The most frequent may be streaks due to planar faults, one of the most common objects studied by electron microscopy. Diffraction patterns are usually sufficient to determine the orientation and the fault vector; the positions and distribution of faults are more easily seen by dark-field microscopy, whereas the detailed atomic arrangement is best studied by high-resolution imaging of the structure [Section 4.3.8 in *IT* C (1999)].

This combination of diffraction and different imaging techniques cannot be applied in the same way to the study of the essentially three-dimensional substitutional local order. Considerable effort has therefore been made to interpret the details of diffuse scattering, leaving the determination of the short-range-order (SRO) parameters usually to X-ray or neutron studies.

Frequently, characteristic shapes or splitting of the diffuse spots from *e.g.* binary alloys are observed. They reflect order extending over many atomic distances, and have been assumed to arise from forces other than the near-neighbour pair forces invoked in the theory of local order. A relationship between the diffuse-scattering distribution and the Fourier transform of the effective atom-pair-interaction potential is given by the ordering theory of Clapp & Moss (1968). An interpretation in terms of long-range forces carried by the conduction electrons was proposed by Krivoglaz (1969). Extensive studies of alloy systems (Ohshima & Watanabe, 1973) show that the separations, m, observed in split diffuse spots from many alloys follow the predicted variation with the electron/atom ratio e/a:

$$m = \left[\frac{12}{\pi}(e/a)\right]^{1/3} t - \sqrt{2},$$

where m is measured along the [110] direction in units of $2a^*$ and t is a truncation factor for the Fermi surface.

A similarity between the location of diffuse maxima and the shape of the Fermi surface has been noted also for other structures, notably some defect rock-salt-type structures. Although this may offer a clue to the forces involved in the ordering, it entails no description of the local structure. Several attempts have been made to formulate principles for building the disordered structure, from small ordered domains embedded in less ordered regions (Hashimoto, 1974), by a network of antiphase boundaries, or by building the structure from clusters with the average composition and coordination (De Ridder *et al.*, 1976). Evidence for such models may be sought by computer simulations, in the details of the SRO scattering as seen in electron diffraction, or in images.

The cluster model is most directly tied to the location of diffuse scattering, noting that a relation between order parameters derived from clusters consistent with the ordered state can be used to predict the position of diffuse scattering in the form of surfaces in reciprocal space, *e.g.* the relation $\cos h + \cos k + \cos l = 0$ for ordering of octahedral clusters in the rock-salt-type structure (Sauvage & Parthé, 1974).

Some of the models imply local fluctuations in order which may be observable either by diffraction from very small regions or by imaging. Microdiffraction studies (Tanaka & Cowley, 1985) do indeed show that spots from 1–1.5 nm regions in disordered $LiFeO_2$ appear on the locus of diffuse maxima observed in diffraction from larger areas.

Imaging of local variations in the SRO structure has been pursued with different techniques (De Ridder *et al.*, 1976; Tanaka & Cowley, 1985; De Meulenaare *et al.*, 1998), *viz*: dark field using diffuse spots only; bright field with the central spot *plus* diffuse spots; lattice image. With domains of about 3 nm or more, high-resolution images seem to give clear indication of their presence and form. For smaller ordered regions, the interpretation becomes increasingly complex: Since the domains will then usually not extend through the thickness of the foil, they cannot be imaged separately. Since image-contrast calculations essentially demand complete specification of the local structure, a model beyond the statistical description must be constructed in order to be compared with observations. On the other hand, these models of the local structure should be consistent with the statistics derived from diffraction patterns collected from a larger volume.

4.2 (*cont.*)

Young, R. A. (1975). Editor. *International discussion meeting on studies of lattice distortions and local atomic arrangements by X-ray, neutron and electron diffraction. J. Appl. Cryst.* **8**, 79–191.

Zernike, F. & Prins, J. A. (1927). *Die Beugung von Röntgenstrahlen in Flüssigkeiten als Effekt der Molekülanordnung. Z. Phys.* **41**, 184–194.

4.3

Allen, L. J., Josefsson, T. W., Lehmpfuhl, G. & Uchida, Y. (1997). *Modeling thermal diffuse scattering in electron diffraction involving higher-order Laue zones. Acta Cryst.* A**53**, 421–425.

Andersson, B. (1979). *Electron diffraction study of diffuse scattering due to atomic displacements in disordered vanadium monoxide. Acta Cryst.* A**35**, 718–727.

Andersson, B., Gjønnes, J. & Taftø, J. (1974). *Interpretation of short range order scattering of electrons; application to ordering of defects in vanadium monoxide. Acta Cryst.* A**30**, 216–224.

Clapp, P. C. & Moss, S. C. (1968). *Correlation functions of disordered binary alloys. II. Phys. Rev.* **171**, 754–763.

Cowley, J. M. (1976*a*). *Diffraction by crystals with planar faults. I. General theory. Acta Cryst.* A**32**, 83–87.

Cowley, J. M. (1976*b*). *Diffraction by crystals with planar faults. II. Magnesium fluorogermanate. Acta Cryst.* A**32**, 88–91.

Cowley, J. M. (1981). *Diffraction physics*, 2nd ed. Amsterdam: North-Holland.

Cowley, J. M. (1988). *Electron microscopy of crystals with time-dependent perturbations. Acta Cryst.* A**44**, 847–853.

Cowley, J. M. (1989). *Multislice methods for surface diffraction and inelastic scattering.* In *Computer simulation of electron microscope diffraction and images*, edited by W. Krakow & M. O'Keefe, pp. 1–12. Worrendale, PA: The Minerals, Metals and Materials Society.

Cowley, J. M. & Fields, P. M. (1979). *Dynamical theory for electron scattering from crystal defects and disorder. Acta Cryst.* A**35**, 28–37.

De Meulenaare, P., Rodewald, M. & Van Tendeloo, G. (1998). *Anisotropic cluster model for the short-range order in Cu_{1-x}–Pd_x-type alloys. Phys. Rev. B*, **57**, 11132–11140.

De Ridder, R., Van Tendeloo, G. & Amelinckx, S. (1976). *A cluster model for the transition from the short-range order to the long-range order state in f.c.c. based binary systems and its study by means of electron diffraction. Acta Cryst.* A**32**, 216–224.

Doyle, P. A. (1969). *Dynamical calculation of thermal diffuse scattering. Acta Cryst.* A**25**, 569–577.

Ferrel, R. A. (1957). *Characteristic energy loss of electrons passing through metal foils. Phys. Rev.* **107**, 450–462.

Fields, P. M. & Cowley, J. M. (1978). *Computed electron microscope images of atomic defects in f.c.c. metals. Acta Cryst.* A**34**, 103–112.

Fisher, P. M. J. (1969). *The development and application of an n-beam dynamic methodology in electron diffraction.* PhD thesis, University of Melbourne. [See also Cowley (1981), ch. 17.]

Freeman, A. J. (1959). *Compton scattering of X-rays from non-spherical charge distributions. Phys. Rev.* **113**, 169–175.

Freeman, A. J. (1960). *X-ray incoherent scattering functions for non-spherical charge distributions. Acta Cryst.* **12**, 929–936.

Fujimoto, F. & Kainuma, Y. (1963). *Inelastic scattering of fast electrons by thin crystals. J. Phys. Soc. Jpn*, **18**, 1792–1804.

Gjønnes, J. (1962). *Inelastic interaction in dynamic electron scattering. J. Phys. Soc. Jpn*, **17**, Suppl. BII, 137–139.

Gjønnes, J. (1966). *The influence of Bragg scattering on inelastic and other forms of diffuse scattering of electrons. Acta Cryst.* **20**, 240–249.

Gjønnes, J. & Høier, R. (1971). *Structure information from anomalous absorption effects in diffuse scattering of electrons. Acta Cryst.* A**27**, 166–174.

Gjønnes, J. & Taftø, J. (1976). *Bloch wave treatment of electron channelling. Nucl. Instrum. Methods*, **133**, 141–148.

Hashimoto, S. (1974). *Correlative microdomain model for short range ordered alloy structures. I. Diffraction theory. Acta Cryst.* A**30**, 792–798.

Høier, R. (1973). *Multiple scattering and dynamical effects in diffuse electron scattering. Acta Cryst.* A**29**, 663–672.

Honjo, G., Kodera, S. & Kitamura, N. (1964). *Diffuse streak diffraction patterns from single crystals. I. General discussion and aspects of electron diffraction diffuse streak patterns. J. Phys. Soc. Jpn*, **19**, 351–369.

Howie, A. (1963). *Inelastic scattering of electrons by crystals. I. The theory of small angle inelastic scattering. Proc. Phys. Soc. A*, **271**, 268–287.

Iijima, S. & Cowley, J. M. (1977). *Study of ordering using high resolution electron microscopy. J. Phys. (Paris)*, **38**, Suppl. C7, 21–30.

International Tables for Crystallography (1999). Vol. C. *Mathematical, physical and chemical tables*, edited by A. J. C. Wilson & E. Prince. Dordrecht: Kluwer Academic Publishers.

Kainuma, Y. (1955). *The theory of Kikuchi patterns. Acta Cryst.* **8**, 247–257.

Krahl, D., Pätzold, H. & Swoboda, M. (1990). *An aberration-minimized imaging energy filter of simple design. Proceedings of the 12th international conference on electron microscopy*, Vol. 2, pp. 60–61.

Krivanek, O. L., Gubbens, A. J., Dellby, N. & Meyer, C. E. (1992). *Design and first applications of a post-column imaging filter. Micros. Microanal. Microstruct. (France)*, **3**, 187–199.

Krivanek, O. L. & Mooney, P. E. (1993). *Applications of slow-scan CCD cameras in transmission electron microscopy. Ultramicroscopy*, **49**, 95–108.

Krivoglaz, M. A. (1969). *Theory of X-ray and thermal neutron scattering by real crystals.* New York: Plenum.

Leapman, R. D., Rez, P. & Mayers, D. F. (1980). *L and M shell generalized oscillator strength and ionization cross sections for fast electron collisions. J. Chem. Phys.* **72**, 1232–1243.

Loane, R. F., Xu, P. R. & Silcox, J. (1991). *Thermal vibrations in convergent-beam electron diffraction. Acta Cryst.* A**47**, 267–278.

Marks, L. D. (1985). *Image localization. Ultramicroscopy*, **18**, 33–38.

Maslen, W. V. & Rossouw, C. J. (1984). *Implications of (e, 2e) scattering electron diffraction in crystals: I–II. Philos. Mag.* A**49**, 735–742, 743–757.

Moliere, G. (1948). *Theory of scattering of fast charged particles: plural and multiple scattering. Z. Naturforsch. Teil A*, **3**, 78–97.

Mori, M., Oikawa, T. & Harada, Y. (1990). *Development of the imaging plate for the transmission electron microscope and its characteristics. J. Electron Microsc. (Jpn)*, **19**, 433–436.

Ohshima, K. & Watanabe, D. (1973). *Electron diffraction study of short-range-order diffuse scattering from disordered Cu–Pd and Cu–Pt alloys. Acta Cryst.* A**29**, 520–525.

Ohtsuki, Y. H., Kitagaku, M., Waho, T. & Omura, T. (1976). *Dechannelling theory with the Fourier–Planck equation and a modified diffusion coefficient. Nucl. Instrum Methods*, **132**, 149–151.

Rez, P., Humphreys, C. J. & Whelan, M. J. (1977). *The distribution of intensity in electron diffraction patterns due to phonon scattering. Philos. Mag.* **35**, 81–96.

Sauvage, M. & Parthé, E. (1974). *Prediction of diffuse intensity surfaces in short-range-ordered ternary derivative structures based on ZnS, NaCl, CsCl and other structures. Acta Cryst.* A**30**, 239–246.

Taftø, J. & Lehmpfuhl, G. (1982). *Direction dependence in electron energy loss spectroscopy from single crystals. Ultramicroscopy*, **7**, 287–294.

Taftø, J. & Spence, J. C. H. (1982). *Atomic site determination using channelling effect in electron induced X-ray emission. Ultramicroscopy*, **9**, 243–247.

Tanaka, N. & Cowley, J. M. (1985). *High resolution electron microscopy of disordered lithium ferrites. Ultramicroscopy*, **17**, 365–377.

Tanaka, N. & Cowley, J. M. (1987). *Electron microscope imaging of short range order in disordered alloys. Acta Cryst.* A**43**, 337–346.

4.3 (*cont.*)

Uyeda, R. & Nonoyama, M. (1968). *The observation of thick specimens by high voltage electron microscopy. Jpn. J. Appl. Phys.* **1**, 200–208.

Van Hove, L. (1954). *Correlations in space and time and Born approximation scattering in systems of interacting particles. Phys. Rev.* **95**, 249–262.

Wang, Z. L. (1995). *Elastic and inelastic scattering in electron diffraction and imaging*. New York: Plenum Press.

Whelan, M. (1965). *Inelastic scattering of fast electrons by crystals. I. Interband excitations. J. Appl. Phys.* **36**, 2099–2110.

Yoshioka, H. (1957). *Effect of inelastic waves on electron diffraction. J. Phys. Soc. Jpn*, **12**, 618–628.

4.4

Aeppli, G. & Bruinsma, R. (1984). *Hexatic order and liquid crystal density fluctuations. Phys. Rev. Lett.* **53**, 2133–2136.

Aeppli, G., Litster, J. D., Birgeneau, R. J. & Pershan, P. S. (1981). *High resolution X-ray study of the smectic A–smectic B phase transition and the smectic B phase in butyloxybenzylidene octylaniline. Mol. Cryst. Liq. Cryst.* **67**, 205–214.

Aharony, A., Birgeneau, R. J., Brock, J. D. & Litster, J. D. (1986). *Multicriticality in hexatic liquid crystals. Phys. Rev. Lett.* **57**, 1012–1015.

Alben, R. (1973). *Phase transitions in a fluid of biaxial particles. Phys. Rev. Lett.* **30**, 778–781.

Als-Nielsen, J., Christensen, F. & Pershan, P. S. (1982). *Smectic-A order at the surface of a nematic liquid crystal: synchrotron X-ray diffraction. Phys. Rev. Lett.* **48**, 1107–1110.

Als-Nielsen, J., Litster, J. D., Birgeneau, R. J., Kaplan, M., Safinya, C. R., Lindegaard, A. & Mathiesen, S. (1980). *Observation of algebraic decay of positional order in a smectic liquid crystal. Phys. Rev. B*, **22**, 312–320.

Bak, P., Mukamel, D., Villain, J. & Wentowska, K. (1979). *Commensurate–incommensurate transitions in rare-gas monolayers adsorbed on graphite and in layered charge-density-wave systems. Phys. Rev. B*, **19**, 1610–1613.

Barois, P., Prost, J. & Lubensky, T. C. (1985). *New critical points in frustrated smectics. J. Phys. (Paris)*, **46**, 391–399.

Beaglehole, D. (1982). *Pretransition order on the surface of a nematic liquid crystal. Mol. Cryst. Liq. Cryst.* **89**, 319–325.

Benattar, J. J., Doucet, J., Lambert, M. & Levelut, A. M. (1979). *Nature of the smectic F phase. Phys. Rev. A*, **20**, 2505–2509.

Benattar, J. J., Levelut, A. M. & Strzelecki, L. (1978). *Etude de l'influence de la longueur moléculaire les charactéristiques des phases smectique ordonnées. J. Phys. (Paris)*, **39**, 1233–1240.

Benattar, J. J., Moussa, F. & Lambert, M. (1980). *Two-dimensional order in the smectic F phase. J. Phys. (Paris)*, **40**, 1371–1374.

Benattar, J. J., Moussa, F. & Lambert, M. (1983). *Two dimensional ordering in liquid crystals: the SmF and SmI phases. J. Chim. Phys.* **80**, 99–107.

Benattar, J. J., Moussa, F., Lambert, M. & Germian, C. (1981). *Two kinds of two-dimensional order: the SmF and SmI phases. J. Phys. (Paris) Lett.* **42**, L67–L70.

Benguigui, L. (1979). *A Landau theory of the NAC point. J. Phys. (Paris) Colloq.* **40**, C3-419–C3-421.

Bensimon, D., Domany, E. & Shtrikman, S. (1983). *Optical activity of cholesteric liquid crystals in the pretransitional regime and in the blue phase. Phys. Rev. A*, **28**, 427–433.

Billard, J., Dubois, J. C., Vaucher, C. & Levelut, A. M. (1981). *Structures of the two discophases of rufigallol hexa-n-octanoate. Mol. Cryst. Liq. Cryst.* **66**, 115–122.

Birgeneau, R. J., Garland, C. W., Kasting, G. B. & Ocko, B. M. (1981). *Critical behavior near the nematic–smectic-A transition in butyloxybenzilidene octylaniline (4O.8). Phys. Rev. A*, **24**, 2624–2634.

Birgeneau, R. J. & Litster, J. D. (1978). *Bond orientational order model for smectic B liquid crystals. J. Phys. (Paris) Lett.* **39**, L399–L402.

Blinc, R. & Levanyuk, A. P. (1986). Editors. *Modern problems in condensed matter sciences, incommensurate phases in dielectrics, 2. Materials.* Amsterdam: North-Holland.

Brisbin, D., De Hoff, R., Lockhart, T. E. & Johnson, D. L. (1979). *Specific heat near the nematic–smectic-A tricritical point. Phys. Rev. Lett.* **43**, 1171–1174.

Brock, J. D., Aharony, A., Birgeneau, R. J., Evans-Lutterodt, K. W., Litster, J. D., Horn, P. M., Stephenson, G. B. & Tajbakhsh, A. R. (1986). *Orientational and positional order in a tilted hexatic liquid crystal phase. Phys. Rev. Lett.* **57**, 98–101.

Brooks, J. D. & Taylor, G. H. (1968). In *Chemistry and physics of carbon*, Vol. 3, edited by P. L. Walker Jr, pp. 243–286. New York: Marcel Dekker.

Bruinsma, R. & Nelson, D. R. (1981). *Bond orientational order in smectic liquid crystals. Phys. Rev. B*, **23**, 402–410.

Caillé, A. (1972). *Remarques sur la diffusion des rayons X dans les smectiques A. C. R. Acad. Sci. Sér. B*, **274**, 891–893.

Carlson, J. M. & Sethna, J. P. (1987). *Theory of the ripple phase in hydrated phospholipid bilayers. Phys. Rev. A*, **36**, 3359–3363.

Chan, K. K., Deutsch, M., Ocko, B. M., Pershan, P. S. & Sorensen, L. B. (1985). *Integrated X-ray scattering intensity measurement of the order parameter at the nematic to smectic-A phase transition. Phys. Rev. Lett.* **54**, 920–923.

Chan, K. K., Pershan, P. S., Sorensen, L. B. & Hardouin, F. (1985). *X-ray scattering study of the smectic-A1 to smectic-A2 transition. Phys. Rev. Lett.* **54**, 1694–1697.

Chan, K. K., Pershan, P. S., Sorensen, L. B. & Hardouin, F. (1986). *X-ray studies of transitions between nematic, smectic-A1, -A2, and -Ad phases. Phys. Rev. A*, **34**, 1420–1433.

Chandrasekhar, S. (1982). In *Advances in liquid crystals*, Vol. 5, edited by G. H. Brown, pp. 47–78. London/New York: Academic Press.

Chandrasekhar, S. (1983). *Liquid crystals of disk-like molecules. Philos. Trans. R. Soc. London Ser. A*, **309**, 93–103.

Chandrasekhar, S., Sadashiva, B. K. & Suresh, K. A. (1977). *Liquid crystals of disk like molecules. Pramana*, **9**, 471–480.

Chapman, D., Williams, R. M. & Ladbrooke, B. D. (1967). *Physical studies of phospholipids. VI. Thermotropic and lyotropic mesomorphism of some 1,2-diacylphosphatidylcholines (lecithins). Chem. Phys. Lipids*, **1**, 445–475.

Chen, J. H. & Lubensky, T. C. (1976). *Landau–Ginzberg mean-field theory for the nematic to smectic-C and nematic to smectic-A phase transitions. Phys. Rev. A*, **14**, 1202–1207.

Chu, K. C. & McMillan, W. L. (1977). *Unified Landau theory for the nematic, smectic A and smectic C phases of liquid crystals. Phys. Rev. A*, **15**, 1181–1187.

Coates, D. & Gray, G. W. (1975). *A correlation of optical features of amorphous liquid–cholesteric liquid crystal transitions. Phys. Lett. A*, **51**, 335–336.

Collett, J. (1983). PhD thesis, Harvard University, USA. Unpublished.

Collett, J., Pershan, P. S., Sirota, E. B. & Sorensen, L. B. (1984). *Synchrotron X-ray study of the thickness dependence of the phase diagram of thin liquid-crystal films. Phys. Rev. Lett.* **52**, 356–359.

Collett, J., Sorensen, L. B., Pershan, P. S. & Als-Nielsen, J. (1985). *X-ray scattering study of restacking transitions in the crystalline-B phases of heptyloxybenzylidene heptylaniline 7O.7. Phys. Rev. A*, **32**, 1036–1043.

Collett, J., Sorensen, L. B., Pershan, P. S., Litster, J., Birgeneau, R. J. & Als-Nielsen, J. (1982). *Synchrotron X-ray study of novel crystalline-B phases in 7O.7. Phys. Rev. Lett.* **49**, 553–556.

Crooker, P. P. (1983). *The cholesteric blue phase: a progress report. Mol. Cryst. Liq. Cryst.* **98**, 31–45.

Davey, S. C., Budai, J., Goodby, J. W., Pindak, R. & Moncton, D. E. (1984). *X-ray study of the hexatic-B to smectic-A phase transition in liquid crystal films. Phys. Rev. Lett.* **53**, 2129–2132.

Davidov, D., Safinya, C. R., Kaplan, M., Dana, S. S., Schaetzing, R., Birgeneau, R. J. & Litster, J. D. (1979). *High-resolution X-ray and light-scattering study of critical behavior associated with the nematic–smectic-A transition in 4-cyano-4′-octylbiphenyl. Phys. Rev. B*, **19**, 1657–1663.